Nanoscale

PAPER

Aluminum based sulfide solid lithium ionic conductors for all solid state batteries†

Cite this: *Nanoscale*, 2014, **6**, 6661

S. Amaresh,[a] K. Karthikeyan,[ab] K. J. Kim,[a] Y. G. Lee[c] and Y. S. Lee*[a]

Received 13th February 2014
Accepted 31st March 2014

DOI: 10.1039/c4nr00804a

www.rsc.org/nanoscale

The present work focuses on the synthesis of lithium ionic conductors based on a Li_2S–Al_2S_3–GeS–P_2S_5 system due to the high ionic conductivity exhibited by the constituents of this system. Mechanical milling for a short duration and a single step heat treatment at a moderate temperature of 550 °C resulted in crystalline powders with high lithium ionic conductivity at room temperature that are comparable to the organic liquid electrolytes. The effect of various aluminum to germanium ratios was studied. Among the samples containing Al : Ge, the ratio of 30 : 70 was found to show high ionic conductivities of 1.7×10^{-3} S cm^{-1} at 25 °C and $\sim 6 \times 10^{-3}$ S cm^{-1} at 100 °C equivalent. The activation energy of this material was significantly less (E_a = 17 kJ mol^{-1}), which can be considered to be the best value among solid electrolytes. The electrochemical stability was analyzed using cyclic voltammetry between −0.3 and 5.0 V and it was found that the voltammetric profile was smooth without any additional current response, due to electrolyte decomposition, or any other side reaction, except a pair of lithium deposition and stripping peaks.

Introduction

Lithium ion batteries (LIBs) with high energy density could be an obvious candidate as a powerful energy source for electric vehicles. Many research groups have focused on high voltage cathode materials, such as $LiCoPO_4$, Li_2CoPO_4F, and $LiNi_{0.5}Mn_{1.5}O_4$,[1–3] in order to improve the energy density of LIBs to a new level for use in modern electric vehicles. However, the important obstacle for operating high voltage batteries was found to be the instability of organic electrolytes with the formation of highly acidic decomposition products during cycling. This resulted in reduced reversibility of batteries, exponential increase in side reactions with highly active lithium, and explosion due to an increase in the temperature of the battery during operation. The above impediments can be overcome with the development of solid state batteries using a solid lithium ion conductor (SLIC) between positive and negative electrode materials, which could eliminate the issues related to liquid electrolytes. It is well known that commercially available organic solvent based liquid electrolytes cannot withstand high environmental temperatures and decompose to form reaction products that react with the electrode components, which could cause serious explosion hazards during cycling. When suitably developed for specific mobile ionic conduction, various applications for solid electrolytes should be found in all energy storage devices and could act as media for conducting ions as well as separators between two different compartments that have materials with varying reaction mechanisms. In this respect, lithium ion conducting solid electrolytes are expected to deliver a high room temperature ionic conductivity and high stability against lithium reactivity.[4]

Besides high ionic conductivity, SLICs were expected to have low electronic conductivity, minimum self-discharge for long shelf life, low electrode corrosion, good thermo-mechanical strength for easy packaging, and good thermal stability in a broad temperature range for a safer operation under various climatic conditions. H. Y. P. Hong first introduced the concept of lithium superionic conductors (LISICONs) and found the highest lithium ionic conductivity of 1.3×10^{-1} S cm^{-1} at an elevated temperature (>300 °C) for $Li_{14}Zn(GeO_4)_4$.[5] $Li_{14}Zn(GeO_4)_4$ belonged to a binary system consisting of Li_4GeO_4 and Li_2ZnGeO_4 end members, while Li_2ZnGeO_4 was isostructural to Li_3PO_4. Improved lithium ion conductivity in the order of 10^{-5} S cm^{-1} at room temperature was observed for materials developed within the composition of the binary system using the additional effect of doping ions such as Ga, Al, and Zr. Meanwhile, Li_4GeO_4–Li_2SO_4 based solid solutions with a γ-Li_3PO_4 structure were found to have reasonably good conductivity at room temperature compared to the corresponding oxide-only counterparts.[6–8]

[a]*Faculty of Applied Chemical Engineering, Chonnam National University, Gwangju 500-757, Korea. E-mail: leeys@chonnam.ac.kr; Fax: +82 62 530 1904; Tel: +82 62 530 1904*

[b]*Department of Mechanical and Materials Engineering, The University of Western Ontario, London, Ontario, N6A 5B9, Canada*

[c]*Power Control Device Research Team, Electronics and Telecommunications Research Institute, Daejeon 305-700, Korea*

† Electronic supplementary information (ESI) available: XRD setup and the equivalent circuit model for resistance calculation. See DOI: 10.1039/c4nr00804a

The development of solid electrolytes was envisioned differently, *i.e.*, by replacing all of the oxides with larger and more polarizable sulfide ions, a new family, named thio-LISICON, was formed.[9] Ternary systems represented by Li_2S–GeS_2–P_2S_5, Li_2S–SiS_2–Al_2S_3, and Li_2S–SiS_2–P_2S_5 were developed as thio-LISICON solid electrolytes and were found to have ionic conductivity in the range of 10^{-4} to 10^{-3} S cm^{-1} at 27 °C. These crystalline powders had lithium ions randomly distributed along the conduction pathway of infinitely running LiS_6 octahedral chains interconnected by LiS_4 tetrahedra.[10] The replacement of Zn in the LISICON framework, with the formula of $Li_{4-2x}Zn_xGeS_4$ with P^{5+} ions to form $Li_{4-x}Ge_{1-x}P_xS_4$, resulted in high conductivity at room temperature due to the vacancies created by aliovalent doping.[11,12] The ionic conductivity of the parent compound Li_4GeS_4 (2×10^{-7} S cm^{-1} at 25 °C) was definitely higher than that of the oxide form, Li_4GeO_4 (3×10^{-10} S cm^{-1} at 110 °C). A similar type of sulfide based glass and glassy ceramics was also conceptualized. Mechanical milling was primarily used to synthesize the amorphous phase of SILCs. The glassy electrolyte of $xLi_2S(100 - x)P_2S_5$ ($75 \leq x \leq 80$) was investigated. Ionic conductivity in the order of 10^{-4} S cm^{-1} was obtained at room temperature.[13] While the most successful inorganic solid electrolyte was $Li_{3x}La_{(2/3)-x}TiO_3$ (LLTO), which had an ionic conductivity of >10^{-3} S cm^{-1} under ambient conditions, this material functions with the help of vacancies created during high temperature heating associated with the loss of lithium during synthesis. The ambiguous nature of vacancy formation and lithium ionic conduction means that LLTO is a less preferred choice for applications.[14] Another class of lithium ion conductors is the inorganic chalcogenide framework (ICF), with the general formula In_xS_y or $M_xIn_yS_z$ (ref. 15) and was represented by the zeolite framework compounds comprising thioindate materials such as ICF-26 and Li_4SnS_4.[15,16] ICFs having high humidity exhibited lithium ionic conductivity in the order of 10^{-2} S cm^{-1}, but the humidity factor restricted ICFs for use in lithium related energy storage devices.

First principle analysis by Ceder *et al.*[18] revealed that higher ionic conductivity and lower activation barrier can be obtained for an aluminum based solid electrolyte system. In addition, cation substitutions such as Si or Sn were not favorable in terms of ionic conductivity, while the aliovalent cation (Al^{3+}) substitution resulted in better performance, which may be due to the larger channel size provided by the substitution for Li^+ diffusion. It was also found that, in spite of the considerably larger channel size obtained using Se anionic substitution, the Li diffusivity is more favorable for sulfides than other anions, such as Se and O, which may be attributed to the critical channel size for Li diffusion and the size of the highly polarizable sulfide ion.[18,19] Recently, aluminum based thio-LISICON systems such as Li_2S–Al_2S_3–SiS_2 and Li_2S–Al_2S_3–P_2S_5 were reported to have room temperature ionic conductivity in the order of 10^{-4} S cm^{-1} with an activation energy of approximately ~35 kJ mol^{-1}.[32,33] Most of the research discussed above on solid electrolytes focused on either a germanium or aluminum based system with phosphorus ions being the primary structural unit for creating a framework structure that is helpful in the movement of Li ions. Motivated by the trend and activity of component ions in the solid electrolyte for Li diffusivity, in this study, we attempted to synthesize a combination of both Al and Ge based Li_2S–Al_2S_3–GeS–P_2S_5 systems with the assumption that the system could result in room temperature (25 °C) ionic conductivities higher than those reported for aluminum based systems and also would increase the stability of the thio-LISICON solid electrolytes against metallic lithium. The primary focus was given to easy synthesis and minimal use of the highly expensive germanium compound; the solid electrolytes thus obtained could satisfy the properties mentioned above and could be applied in solid state lithium secondary batteries.

Experimental

High purity chemicals, Li_2S, GeS, S, P_2S_5, and Al_2S_3 (Sigma-Aldrich, USA), were used for the preparation of solid state lithium ion conductors. All the chemicals were handled under a high purity argon atmosphere throughout the study to ensure a moisture free environment and to prevent decomposition of the materials in reaction with external moisture and oxygen. The phosphorus and sulfur contents were fixed as $P = 2$ and $S = 12$. The aluminum to germanium composition was maintained at different ratios from 100 : 0 to 10 : 90. The precursor powders were weighed accurately into a zirconia pot and were carefully sealed with alumina balls. The total mass of the powders was 1.5 g for each batch. Mechanical milling was carried out using high energy planetary ball milling equipment (Pulverisette 6, Fritsch, Germany) at 500 rpm for 30 min. After ensuring the proper mixing of the precursor powders, the dark brown sample was pelletized at 380 MPa. The compressed pellet was then carefully loaded into the reactor under an argon atmosphere. An optimum synthetic temperature of 550 °C was selected and the steady state holding time was about 8 h with natural cooling to ramp down the temperature after the heating period.

The synthesized pellets were ground using a mortar and pestle before being used for various characterization studies. A specialized CR2032 cell construction as provided in the ESI (Fig. S1†) was used for X-ray diffraction (XRD) measurement using Cu Kα (1.5406 Å) radiation in a D/MAX Ultima III (Rigaku, Japan) instrument in the diffraction angle range of 15–60°. A thin pellet of 1–2 mm thickness of 10 mm diameter was prepared under a pressure of 380 MPa and non-blocking electrodes were used on both sides of the pellet during the ionic conductivity measurement. Potentiostatic impedance was measured in a dry argon atmosphere at a constant voltage of 0.1 V from 1 MHz to 25 Hz at various steady state temperatures using a precise LCR meter (4284A, HP, USA). The sample was equilibrated in the specified temperatures for a minimum of 1 h before measurement. The conductivity was determined using the complex impedance analysis. The ionic conductivity of the sample was calculated using the formula $\sigma = t/(AR)$, where t is the thickness of the pellet, A is the area of the non-blocking electrode used, and R is the resistance obtained during impedance measurement. Cyclic voltammetry (CV) was performed using a simple two-probe cell with a stainless steel plate as a working electrode and lithium foil acted as a counter

 This journal is © The Royal Society of Chemistry 2014

electrode at a scanning rate of 5 mV s^{-1} between −0.3 V and 5.0 V using an electrochemical workstation (Bio Logic, SP-150, France). Chrono-amperometric analysis was carried out to determine the lithium transference number under an applied voltage of 0.5 V, using a symmetric cell holding the solid electrolyte between non-blocking lithium electrodes. Impedance measurement was performed before and after chrono-amperometric measurement in the frequency range of 1 MHz to 50 Hz.

Results and discussion

The schematic diagram explaining the simple synthesis process of lithium solid ionic conductors containing various combination of the Al : Ge ratio is shown in Fig. 1 (see Experimental section for more details). The synthesis process involves ball milling the precursor powders for a short duration in order to mix the constituents at a molecular level. In the second step, the milled powder was subjected to a process called densification, wherein the contact between the particles is established by pelletizing under high pressure. Finally, the pellet is treated at a moderate temperature (550 °C) for obtaining the crystalline phase. The obtained single phase powders were ground before being used for various characterization techniques. The advantages of the synthesis process are as follows: (i) the synthesis step involves a single step heating, unlike an earlier report where the solid electrolyte pellet was re-heated at 500 °C before ionic conductivity measurement.[17] (ii) The synthesis does not involve high heating temperatures and long milling time.[10,25] The usage of GeS instead of GeS_2 has reduced the cost of the starting materials to a considerable quantity.

Fig. 2 shows X-ray diffraction patterns of samples synthesized with various ratios of aluminum and germanium as starting materials. The XRD patterns shown in Fig. 2(a) were obtained using a CR 2032 coin cell setup made in-house as given in the ESI (Fig. S1).† Because the main objective of this work was to check the effect of germanium on the Li–Al–P–S system, a compositional balance was intended so that the ionic conductivity would not be disturbed with the constructive

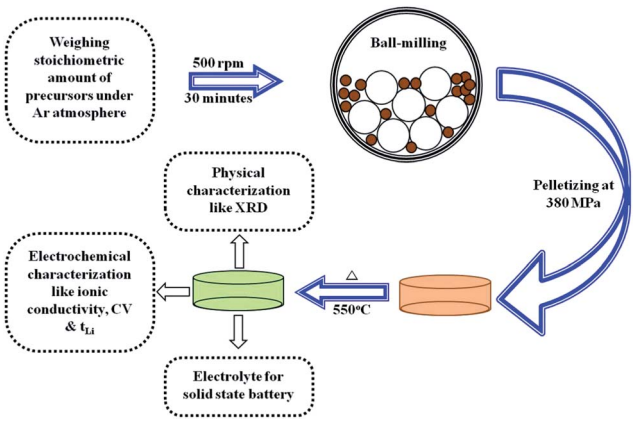

Fig. 1 Schematic diagram illustrating the simple solid state synthesis of the thio-LISICON solid electrolyte. The steps involved in the entire process were carried out in an argon environment.

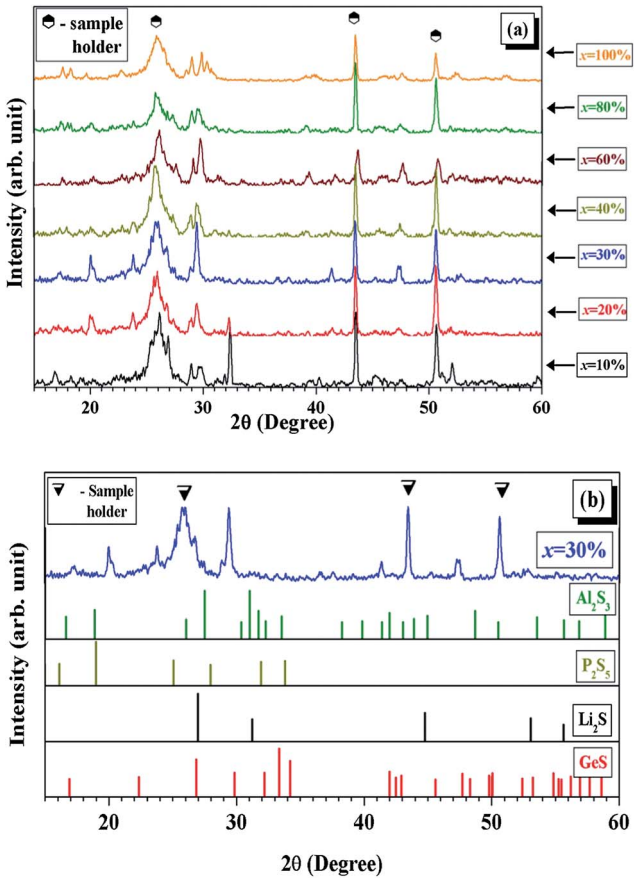

Fig. 2 (a) X-ray diffraction pattern of the sample synthesized with different Al : Ge ratios. The *X* values represent the composition of Al ions. (b) Comparison of reflections of starting materials with the LAGPS-30% sample for any possible impurities.

modification on synthesis methodology. The composition of the $(5 - x)Li_2S$–$(x)Al_2S_3$–$(1 - 2x)GeS$–P_2S_5 (LAGPS) system was selected such that $x = 0.5$–0.05 determines the moles of starting materials to be used for solid electrolyte synthesis. We are reporting the combination of Al–Ge–P based sulfide solid electrolytes for the first time, which are expected to replace the present solid electrolytes in terms of ionic conductivity and stability due to the compatibility of aluminum against the lithium metal anode.[36] A particular trend in the crystal formation shown in Fig. 2(a) was noted when the aluminum composition was decreased from 100 to 10%. If the concentration is maintained in the range of 100–30%, the effect of Al_2S_3 was dominant over GeS. This resulted in splitting of the peak at 29° and the formation of a phase similar to the mixture of thio-LISICON I and III analogues.[35] At lower concentrations, namely 20% and 10%, dominant peaks at 28–30° were formed along with low intensity peaks at 20–24° and the phase was moving towards the formation of the thio-LISICON I analogue.[35] In particular, when the concentration reached an Al : Ge ratio of 30 : 70, the XRD pattern was exactly the same as that of the Li–Ge–P–S (LGPS) system reported by Hassoun *et al.*[21] It was therefore assumed that the LAGPS system with an Al : Ge ratio of 30 : 70 has a tetragonal symmetry. In this regard, LAGPS-30%

was expected to have an ionic conductivity value equivalent to that of the LGPS system. The stoichiometric formula of the resultant system can be written as $Li_{9.7}Al_{0.3}Ge_{0.7}P_2S_{12}$ (LAGPS-30%).

The phase formed with different compositions mentioned above was checked for reflections from starting materials. Specifically, the diffraction reflection of the LAGPS-30% sample was compared with that of the Li_2S (JCPDS # 26-1188), Al_2S_3 (JCPDS # 47-1313), GeS (JCPDS # 51-1168), and P_2S_5 (JCPDS # 50-0813) starting materials as shown in Fig. 2(b). The observation from Fig. 2(b) confirmed the formation of a new phase and the precursors were converted without trace. The effective ionic radius of the Al^{3+} ion (53.5 pm) was comparable to that of the Ge^{4+} ion (53 pm).[28] As a result, it was believed that the size and number of ions present in the LAGPS system were responsible for the formation of a phase similar to the LGPS crystal. The LGPS system has redundant pathways perpendicular to the main Li^+ channels and consequently the system is robust even at high defect concentration that could be created due to the heat treatment temperature, volume expansion by anion reorientation, or vacancy creation with aliovalent doping.[19,20] In addition, the aliovalent cation doping was intended to reduce activation energy barriers and to increase conductivity to some degree.[18] The particular composition exhibited by the LAGPS-30% sample uses a lower amount of germanium, replacing it with aluminum ions, and a 3% reduction in the usage of lithium than the LGPS system, thus decreasing the overall cost of the solid electrolyte. Therefore, the LAGPS systems achieved in this study are of particular interest for low cost all solid state batteries.

Nyquist plots resulting from impedance spectroscopy measurements were used for calculating the ionic conductivity of all the samples. The bulk and/or grain boundary conduction, a common phenomenon in oxide based solid electrolytes, had to be taken into account whenever the Nyquist plot possesses two or more arcs. Instead, the single arc obtained for sulfide based solid electrolytes can be directly related to the ionic conductivity contribution of the samples. Alternatively, the equivalent circuit given in Fig. S2 (ESI†) was used for fitting the impedance plots. The highest ionic conductivity among the synthesized samples was obtained for $Li_{9.7}Al_{0.3}Ge_{0.7}P_2S_{12}$ with values of $\sim 1.7 \times 10^{-3}$ S cm^{-1} at 25 °C and $\sim 6.0 \times 10^{-3}$ S cm^{-1} at 100 °C. The obtained ionic conductivity values at room temperature are compared with the reported sulfide electrolytes based on aluminum. The attempt by Murayama[11] to replace the Li–Si–P–S system with the Li–Al–Si–S system resulted in an ionic conductivity drop to 10^{-7} S cm^{-1} from 10^{-4} S cm^{-1} at room temperature, thus emphasizing the importance of P atoms in governing the lithium ionic conductivity. The amorphous type solid electrolytes based on Li–Al–P–S exhibited a maximum conductivity of 6×10^{-4} S cm^{-1}.[32] However, in this study, the LAGPS solid electrolyte showed higher lithium ionic conduction (1.7×10^{-3} S cm^{-1}) than the above mentioned systems and can be comparable to the LGPS system, but uses a lower quantity of highly expensive germanium. The trend in ionic conductivity values was found to increase from the 100% aluminum content

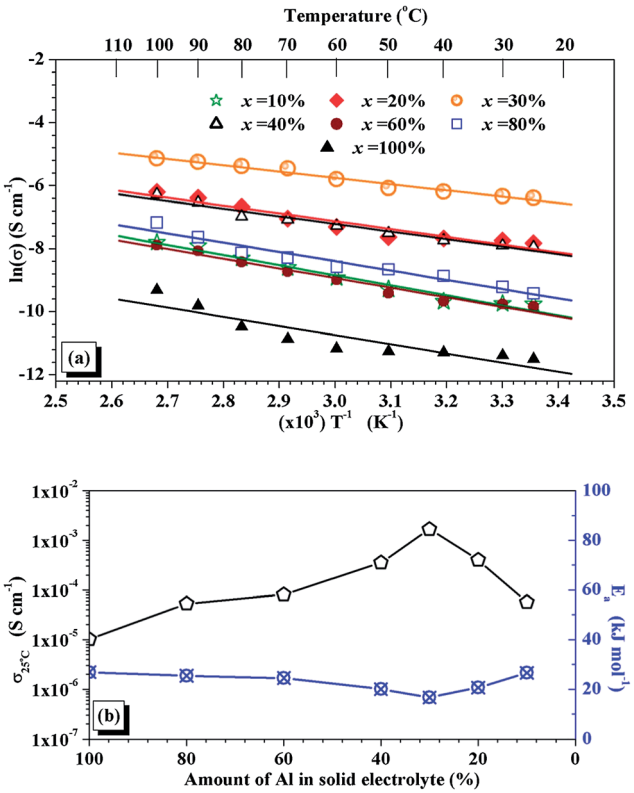

Fig. 3 (a) Ionic conductivities of LAGPS samples in the form of the Arrhenius plot measured from 25 °C to 100 °C. (b) The room temperature (25 °C) ionic conductivities and calculated activation energies of LAGPS samples.

until the composition reached 30% aluminum, and a decreasing trend then appeared as can be seen in Fig. 3(b).

The temperature dependence of the various lithium ion conductors, represented as the Arrhenius plots, is shown in Fig. 3(a). The activation energy of the samples was calculated using the Arrhenius equation $\sigma T = \sigma_o \exp(-E_a/RT)$, where σ is the ionic conductivity of the sample, T is the temperature of conductivity measurement, E_a is the activation energy, and R is the gas constant. The slope of the Arrhenius plots changed to a lesser extent depending upon the composition of the solid electrolyte and temperature; hence the activation energy is directly proportional to the slope. Fig. 3(b) presents the ionic conductivity of all the samples at ambient temperature and the corresponding calculated activation energies. As expected, the activation energies do not vary and the range was within 17–27 kJ mol^{-1}, while the ionic conductivity at 25 °C varied from 1×10^{-5} S cm^{-1} to 1.7×10^{-3} S cm^{-1}. For example, $\sigma_{25\ °C}$ of the samples containing an Al content of 10%, 20%, 40%, 60%, 80%, and 100% was 5.7×10^{-5} S cm^{-1}, 4×10^{-4} S cm^{-1}, 3.5×10^{-4} S cm^{-1}, 8×10^{-5} S cm^{-1}, 5.3×10^{-5} S cm^{-1}, and 1.01×10^{-5} S cm^{-1}, respectively. Meanwhile, the respective activation energies of these samples were 26.6, 20.6, 20, 24.5, 25.4, and 26.8 kJ mol^{-1}, following a similar trend to that of ionic conductivity. Additionally, the XRD and conductivity results emphasized that the microstructure of the sample was very

This journal is © The Royal Society of Chemistry 2014

important for exhibiting rapid Li^+ diffusion and the presence of germanium helps in increasing the ionic conductivity.

It is worth noting that the stoichiometric ratio of lithium in the sample was reduced to a lower value than the LGPS system,[17] which resulted in lower ionic conductivity, although the results of ionic conductivity in this study were satisfactory. An attempt was also made to analyze the effect of the additional lithium ion content using the LAGPS-30% system. The outcome of the further increase in the lithium ion content, without altering all other components, was unexpected and resulted in decreased ionic conductivity values to as low as $\sim 1 \times 10^{-4}$ S cm^{-1} at 25 °C until a maximum of 13% increase of lithium content from the original value. It was believed that the combined effect of aluminum and germanium has the best combination at 30 : 70 and thus the channel size of the LAGPS crystal was optimum for better Li^+ diffusion at this composition. The ionic conductivity and activation energies obtained for the LAGPS system of solid electrolytes could be considered to be better than some of the solid electrolytes such as the Li–P–O–S system (7×10^{-4} S cm^{-1}),[27] Li–Ge–Ga–S system (6.5×10^{-5} S cm^{-1}),[29] Li–P–S system (10^{-4} S cm^{-1}),[30] Li–Si–S system (10^{-4} S cm^{-1}),[30] Li–Al–S system (3.4×10^{-5} S cm^{-1}),[30] Li–P–S–Se system (6×10^{-4} S cm^{-1}),[31] Li–Al–P–S (6×10^{-4} S cm^{-1}),[32] Li–Al–Si–S system (6.7×10^{-5} S cm^{-1}),[33] Li_4SnS_4 (6×10^{-5} S cm^{-1}),[34] and most of the other electrolytes like $Li_{3x}La_{2/3-x}TiO_3$ (5×10^{-4} S cm^{-1}), $Li_5La_3Ta_2O_{12}$ (10^{-4} S cm^{-1}), $Li_{1+x}Ti_{2-x}Al_x(PO_4)_3$ (3×10^{-4} S cm^{-1}), $Li_{1+x}Al_xGe_{2-x}(PO_4)_3$ (1.9×10^{-3} S cm^{-1}) and $LiTi_{0.5}Zr_{1.5}(PO_4)_3$ (2×10^{-6} S cm^{-1}).[14,37]

Chrono-amperometric measurement for determining the lithium transference number was performed by constructing a Li/LAGPS-30% pellet/Li cell; the measurement was conducted at room temperature. The results are shown in Fig. 4. A small potential applied to a solid electrolyte sandwiched between the two non-blocking electrodes leads to a decrease in the current until a steady-state value is reached. The ratio between the initial current and the steady state current resulted in the direct calculation of the transference number. In a practical cell, under the influence of a controlled potential, the process at the surface of the electrolyte is charge transfer and accumulation of ions at the surface of the electrolyte–electrode interface. The result is the formation of a passivating layer, which imposed additional resistance, and the resistance will increase with time depending upon the amount of ionic charge. Hence, impedance measurements were performed in the cell before and after the chrono-amperometric analysis for computing the intrinsic resistance developed due to the passivating film formation.[22] The polarization curve, together with the impedance spectrum obtained for the 30% aluminum sample, is shown in Fig. 4. The lithium transference number (t_{Li+}) was calculated from the formula proposed by Bruce *et al.*[22,23] as follows:

$$t_{Li^+} = \frac{I_{final}\,(V - I_{ini}R_{ini})}{I_{ini}\,(V - I_{final}R_{final})}$$

The variables were represented as follows: V is the applied voltage; I_{ini} and I_{final} are the initial and steady state current responses obtained during DC polarization measurement. Interfacial resistances (R_{ini} and R_{final}) were obtained from the impedance spectra recorded immediately before and immediately after the DC polarization study. The diameter of the semicircle was approximately equal to the resistance; however, the exact value was obtained from the deconvolution of the impedance spectrum. The deconvolution of the impedance spectrum was based on the equivalent circuit that involved two sub-circuits of resistance and constant phase element in parallel, connected in series with the electrolytic resistance. The constant phase element was used due to the fractal nature of composition, current distribution, and roughness of the electrolyte. The electrolytes with a low transference number would result in affecting the operation of the battery due to the increased polarization that reduces the rate capability and safety of the battery. The calculated t_{Li+} for the 30% aluminum sample (LAGPS-30%) was 0.99 and the predominant ionic conductive nature of the electrolyte made the LAGPS-30% sample a favorable candidate as a solid electrolyte for lithium solid state batteries. In comparison, the t_{Li+} of conventional organic electrolytes having $LiPF_6$, $LiBF_4$, LiTFSI and $LiClO_4$ dissolved in various solvents like ethylene carbonate (EC), dimethyl carbonate (DMC), propylene carbonate (PC) and acetonitrile (AN) was in the range of 0.29–0.55.[38] For example, the t_{Li+} of 1 M $LiPF_6$ in EC/DMC is 0.21, 1 M $LiBF_4$ in PC/DMC is 0.29, LiTFSI in DMC (1/20 = solvent/salt) is 0.49 and 0.055 M $LiClO_4$ in AN is 0.39.[38]

The electrochemical stability of the electrolyte was evaluated using the traditional cyclic voltammetry experiment. The CV was recorded using a cell setup consisting of a Li/LAGPS-30% sample/stainless steel plate. The stainless steel plate was used as a counter electrode, while the Li foil acted as a working electrode. Fig. 5 presents the typical Li deposition and stripping reactions at the stainless steel electrode of the cell containing a lithium ionic conductor. The process followed a cathodic sweep first for Li deposition and then the anodic sweep for Li stripping. The cathodic current peak was obtained at −0.3 V and the

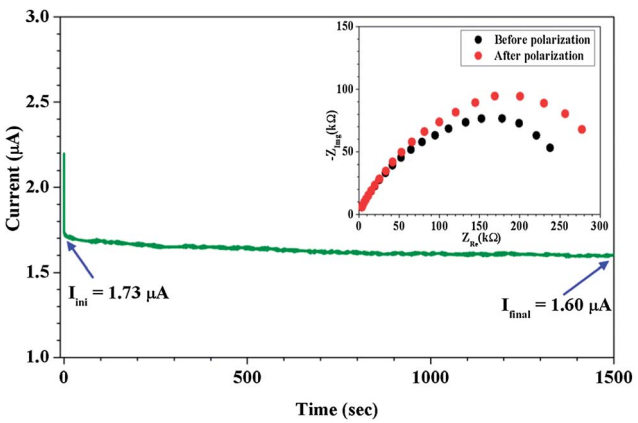

Fig. 4 Chrono-amperometric experiment of the LAGPS-30% sample for determining the lithium transference number under an applied voltage of 0.5 V. The inset shows the impedance taken just before and immediately after the DC polarization experiment.

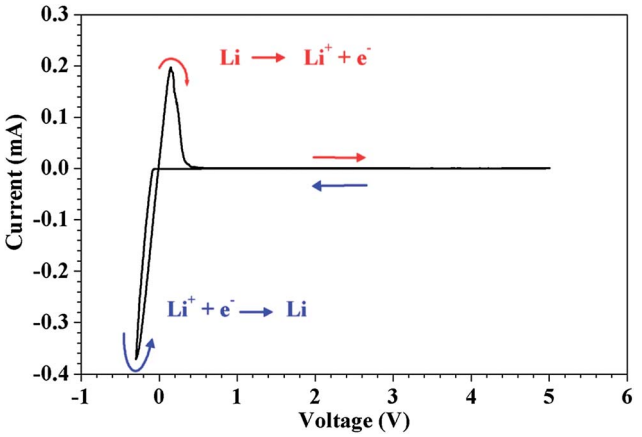

Fig. 5 The electrochemical stability of the LAGPS-30% sample displayed using cyclic voltammetry at a 5 mV s^{-1} scan rate between −0.3 V and 5.0 V.

anodic current peak was at +0.13 V and represented the reactions $Li^+ + e^- \rightarrow Li$ and $Li \rightarrow Li^+ + e^-$, respectively. The current response due to the decomposition of the solid electrolyte was not observed in the CV scan until 5 V, unlike the organic liquid electrolytes in which the apparent sharp or broad peaks representing the decomposition products could be found.[24] The weak anodic response related to the oxidation of free S^{2-} ions between 0 and 4 V found in Li_2S–P–S,[25] $66.7Li_2S{\cdot}33.3P_2S_5$,[26] $80Li_2S{\cdot}20P_2S_5$ (ref. 27) and $80Li_2S{\cdot}19P_2S_5{\cdot}1P_2O_5$ (ref. 27) glass ceramics was not observed in the solid electrolyte synthesized in the present work, because of the presence of aluminum, which could form a stable interface between the electrolyte and metallic lithium. Therefore, the LAGPS-30% sample was found to be stable beyond the operating voltages of commercial organic electrolytes and can be employed with high voltage cathode materials. Additionally, the ionic conductivity of the LAGPS-30% sample in contact with metallic lithium electrodes for 48 h was tested. The ionic conductivity observed at room temperature after 48 h was 1.1×10^{-3} S cm^{-1}, which confirmed the stability of the Al based thio-LISICON solid electrolyte against metallic lithium.

Conclusion

In summary, a series of solid electrolytes having a composition $(5 - x)Li_2S$–$(x)Al_2S_3$–$(1 - 2x)GeS$–P_2S_5 (LAGPS) such that $x = 0.5$–0.05 was synthesized. The obtained ionic conductivity for the 30% aluminum containing sample (1.7×10^{-3} S cm^{-1}) was one of the best values and could be comparable to that of the organic liquid electrolytes. The effective size and ratio of ions between Al and Ge were responsible for the high ionic conductivity observed in the aluminum doped LAGPS system. The synthesis of the LAGPS sample involved a single step heat treatment method and hence could be scaled up effortlessly for mass production in industry. The present example illustrated the effect of aliovalent ion doping on the ionic conductivity and activation energy of the crystalline solid electrolytes. The high lithium diffusivity found can be utilized to fabricate lithium based solid state batteries or batteries with hybrid electrolytes that would enhance the overall energy density, thereby making lithium batteries safe and able to be used for various high energy applications.

Acknowledgements

This work was supported by the Energy Efficiency and Resources R&D program (20112010100150) under the Ministry of Knowledge Economy, Republic of Korea.

References

1 B. Scrosati, K. M. Abraham, W. V. Schalkwijk and J. Hassoun, *Lithium batteries: advanced technologies and applications*, John Wiley & Sons, New Jersey, 2013, ch. 7.
2 C. M. Julien and A. Mauger, *Ionics*, 2013, **19**, 951–988.
3 S. Amaresh, K. Karthikeyan, K. J. Kim, M. C. Kim, K. Y. Chung, B. W. Cho and Y. S. Lee, *J. Power Sources*, 2013, **244**, 395–402.
4 G. Adachi, N. Imanaka and H. Aono, *Adv. Mater.*, 1996, **8**, 127–135.
5 H. Y.-P. Hong, *Mater. Res. Bull.*, 1978, **13**, 117–124.
6 J. G. Kamphorst and E. E. Hellstrom, *Solid State Ionics*, 1980, **1**, 187–197.
7 T. Y. Ayyub and W. Bogusz, *Solid State Ionics*, 1989, **36**, 247–249.
8 M. A. K. L. Dissanayake, R. P. Gunawardane, A. R. West, G. K. R. Senadeera, P. W. S. K. Bandaranayake and M. A. Careem, *Solid State Ionics*, 1993, **62**, 217–223.
9 R. Kanno, T. Hata, Y. Kawamoto and M. Irie, *Solid State Ionics*, 2000, **130**, 97–104.
10 R. Kanno and M. Murayama, *J. Electrochem. Soc.*, 2001, **148**, A742–A746.
11 M. Murayama, R. Kanno, M. Irie, S. Ito, T. Hata, N. Sonoyama and Y. Kawamoto, *J. Solid State Chem.*, 2002, **168**, 140–148.
12 M. Murayama, R. Kanno, Y. Kawamoto and T. Kamiyama, *Solid State Ionics*, 2002, **154–155**, 789–794.
13 F. Mizuno, T. Ohtomo, A. Hayashi, K. Tadanaga and M. Tatsumisago, *Solid State Ionics*, 2006, **177**, 2753–2757.
14 P. Knauth, *Solid State Ionics*, 2009, **180**, 911–916.
15 N. Zheng, X. Bu and P. Feng, *Nature*, 2003, **426**, 428–432.
16 T. Kaib, S. Haddadpour, M. Kapitein, P. Bron, C. Schröder, H. Eckert, B. Roling and S. Dehnen, *Chem. Mater.*, 2012, **24**, 2211–2219.
17 N. Kamaya, K. Homma, Y. Yamakawa, M. Hirayama, R. Kanno, M. Yonemura, T. Kamiyama, Y. Kato, S. Hama, K. Kawamoto and A. Mitsui, *Nat. Mater.*, 2011, **10**, 682–686.
18 S. P. Ong, Y. Mo, W. D. Richards, L. Miara, H. S. Lee and G. Ceder, *Energy Environ. Sci.*, 2013, **6**, 148–156.
19 S. Adams and R. P. Rao, *J. Mater. Chem.*, 2012, **22**, 7687–7691.
20 Y. Mo, S. P. Ong and G. Ceder, *Chem. Mater.*, 2012, **24**, 15–17.
21 J. Hassoun, R. Verrelli, P. Reale, S. Panero, G. Mariotto, S. Greenbaum and B. Scrosati, *J. Power Sources*, 2013, **229**, 117–122.

This journal is © The Royal Society of Chemistry 2014

22 J. Evans, C. A. Vincent and P. G. Bruce, *Polymer*, 1987, **28**, 2324–2328.
23 P. G. Bruce, J. Evans and C. A. Vincent, *Solid State Ionics*, 1988, **28–30**, 918–922.
24 C. Buhrmester, J. Chen, L. Moshurchak, J. Jiang, R. L. Wang and J. R. Dahn, *J. Electrochem. Soc.*, 2005, **152**, A2390–A2399.
25 F. Mizuno, T. Ohtomo, A. Hayashi, K. Tadanaga and M. Tatsumisago, *Solid State Ionics*, 2006, **177**, 2753–2757.
26 N. Machida, H. Yamamoto and T. Shigematsu, *Chem. Lett.*, 2004, **33**, 30–32.
27 T. Ohtomo, F. Mizuno, A. Hayashi, K. Tadanaga and M. Tatsumisago, *J. Power Sources*, 2005, **146**, 715–718.
28 R. D. Shannon, *Acta Crystallogr., Sect. A: Cryst. Phys., Diffr., Theor. Gen. Crystallogr.*, 1976, **A32**, 751–767.
29 R. Kanno, T. Hata, Y. Kawamoto and M. Irie, *Solid State Ionics*, 2000, **130**, 97–104.
30 A. Hayashi, *J. Ceram. Soc. Jpn.*, 2007, **115**, 110–117.
31 J. H. Kim, Y. S. Yoon, M. Y. Eom and D. W. Shin, *Solid State Ionics*, 2012, **225**, 626–630.
32 Y. Ooura, N. Machida, M. Naito and T. Shigematsu, *Solid State Ionics*, 2012, **225**, 350–353.
33 A. Hayashi, T. Fukuda, H. Morimoto, T. Minami and M. Tatsumisago, *J. Mater. Sci.*, 2004, **39**, 5125–5127.
34 T. Kaib, S. Haddadpour, M. Kapitein, P. Bron, C. Schröder, H. Eckert, B. Roling and S. Dehnen, *Chem. Mater.*, 2012, **24**, 2211–2219.
35 R. Kanno and M. Murayama, *J. Electrochem. Soc.*, 2001, **148**, A742–A746.
36 R. Kanno, M. Murayama, T. Inada, T. Kobayashi, K. Sakamoto, N. Sonoyama, A. Yamada and S. Kondo, *Electrochem. Solid-State Lett.*, 2004, **7**, A455–A458.
37 J. W. Fergus, *J. Power Sources*, 2010, **195**, 4554–4569.
38 H. J. Gores, J. Barthel, S. Zugmann, D. Moosbauer, M. Amereller, R. Hartl and A. Maurer, in *Handbook of Battery Materials*, Wiley-VCH Verlag GmbH & Co., Germany, 2nd edn, 2011, ch. 17, pp. 525–626.

This journal is © The Royal Society of Chemistry 2014